Mechanism of Formation of Silver *N*-Heterocyclic Carbenes Using Silver Oxide: A Theoretical Study

Joseph M. Hayes,[†] Mónica Viciano,[‡] Eduardo Peris,*[,‡] Gregori Ujaque,[†] and Agustí Lledós*[,†]

Departament de Química, Universitat Autònoma de Barcelona, 08193 Bellaterra, Catalonia, Spain, and Departamento de Química Inorgánica y Orgánica, Universitat Jaume I, Avda. Vicente Sos Baynat s/n, 12071 Castellón, Spain

Received September 7, 2007

The reasons for the efficiency of the silver oxide route in the synthesis of Ag(I) *N*-heterocyclic carbene complexes have been investigated by means of DFT calculations. A general reaction system that incorporates two *N*,*N*-dimethyl imidazolium cations, two iodides as the counterions, Ag_2O, and dichloromethane solvent was considered. Exploration of several pathways for the formation of the two silver−NHC cations gives a clear picture for the reaction mechanism. The favored route involves a barrierless and very exergonic deprotonation of the first imidazolium followed by a low barrier and also exergonic metalation, affording the first silver−NHC. The second imidazolium assists these two steps stabilizing intermediates and the transition state by the formation of a strong $C_{imidazolium}$−H···OAg hydrogen bond. The formed [R_2NHC]−AgI then diffuses in the solution, while silver hydroxide deprotonates the second imidazolium salt in a slightly endergonic process. After metalation, the second silver−NHC is obtained. The overall reaction is thermodynamically driven, the conversion of two imidazolium salts to two silver carbenes entailing a system stabilization of more than 70 kcal mol^{-1}. As the acid−base reaction between the imidazolium salt and the silver base plays a key role in the process, pK_a calculations were performed to compare the basicity of the *N*-heterocyclic carbene with those of the silver bases Ag_2O, AgOH, and AgOAc. From the pK_a values obtained, the advantage of silver oxide in the generation of silver carbenes is attributed to its stronger basicity.

Introduction

The preparation and use of carbene ligands in organometallic chemistry is currently an extremely hot topic with a number of reviews published very recently describing their importance.[1] *N*-Heterocyclic-carbene ligands (NHCs) have been shown to rival the until now ubiquitous phosphine ligands in their ability to bind metals (both transition and main group metals) and have a major application in the design of enhanced transition metal catalysts. The easy access to NHC-precursors has allowed the fine-tuning of the steric and electronic properties of the ligands obtained. The wide versatility of NHCs also implies the coordination to a large series of metals in different oxidation states. Unlike phosphines, the coordination of NHCs to metals requires the activation or deprotonation of a precursor, thus making NHC-based complexes relatively less accessible than the analogous phosphine compounds. One of the most effective routes for the generation of the *N*-heterocyclic carbene is the reaction of an imidazolium salt with a silver base, producing a Ag(I)−NHC compound.[2] The carbene can then be transmetalated to a transition metal complex,[2,3] thus generating the desired M−NHC compound.

In the generation of the silver−carbene, a variety of silver compounds can be employed, such as Ag_2O,[4] AgOAc,[5] and Ag_2CO_3.[6] Among them, silver oxide is the most commonly used.[2]

* To whom correspondence should be addressed. E-mail: agusti@klingon.uab.es (A.L.); eperis@qio.uji.es (E.P.).

[†] Universitat Autònoma de Barcelona.

[‡] Universitat Jaume I.

(1) Recent reviews: (a) Cornils, B.; Herrmann, W. A. *J. Catal.* **2003**, *216*, 23. (b) Perry, M. C.; Burgess, K. *Tetrahedron: Asymmetry* **2003**, *14*, 951. (c) Herrmann, W. A.; Öfele, K.; von Preysing, D.; Schneider, S. K. *J. Organomet. Chem.* **2003**, *687*, 229. (d) Chui, J. K. W.; Ramnial, T.; Clyburne, J. A. C. *Comments Inorg. Chem.* **2003**, *24*, 165. (e) Cesar, V.; Bellemin-Laponnaz, S.; Gade, L. H. *Chem. Soc. Rev.* **2004**, *33*, 619. (f) Cavell, K. J.; McGuinness, D. S. *Coord. Chem. Rev.* **2004**, *248*, 671. (g) Peris, E.; Crabtree, R. H. *Coord. Chem. Rev.* **2004**, *248*, 2239. (h) Crudden, C. M.; Allen, D. P. *Coord. Chem. Rev.* **2004**, *248*, 2247. (i) Katz, T. J. *Angew. Chem., Int. Ed.* **2005**, *44*, 3010. (j) Dragutan, I.; Dragutan, V.; Delaude, L.; Demonceau, A. *Arkivoc* **2005**, *10*, 206. (k) Lin, I. J. B.; Vasam, C. S. *Can. J. Chem.* **2005**, *83*, 812. (l) Mata, J.; Poyatos, M.; Peris, E. *Coord. Chem. Rev.* **2007**, *251*, 841.

(2) Recent reviews on silver *N*-heterocyclic carbenes: (a) Lin, I. J. B.;Vasam, C. S. *Comments Inorg. Chem.* **2004**, *25*, 75. (b) Garrison, J. C.; Youngs, W. J. *Chem. Rev.* **2005**, *105*, 3978. (c) Lin, I. J. B.; Vasam, C. S. *Coord. Chem. Rev.* **2007**, *251*, 642. (d) Kascatan-Nebioglu, A.; Panzner, M.; Tessier, C. A.; Cannon, C. L.; Youngs, W. J. *Coord. Chem. Rev.* **2007**, *251*, 884.

(3) (a) McGuinness, D. S.; Cavell, K. J. *Organometallics* **2000**, *19*, 741. (b) Lee, K. M.; Wang, H. M.; Lin, I. B. J. *J. Chem. Soc., Dalton Trans.* **2002**, 2852. (c) Schneider, S. K.; Herrmann, W. A.; Herdtweck, E. *Z. Anorg. Allg. Chem.* **2003**, *629*, 2363. (d) Simons, R. S.; Custer, P.; Tessier, C. A.; Youngs, W. J. *Organometallics* **2003**, *22*, 1979. (e) Chianese, A. R.; Li, X. W.; Janzen, M. C.; Faller, J. W.; Crabtree, R. H. *Organometallics* **2003**, *22*, 1663. (f) Bonnet, L. G.; Douthwaite, R. E.; Hodgson, R.; Houghton, J.; Kariuki, B. M.; Simonovic, S. *Dalton Trans.* **2004**, 3528. (g) Mata, J. A.; Chianese, A. R.; Miecznikowski, J. R.; Poyatos, M.; Peris, E.; Faller, J. W.; Crabtree, R. H. *Organometallics* **2004**, *24*, 1253. (h) de Frémont, P.; Scott, N. M.; Stevens, E. D.; Nolan, S. P. *Organometallics* **2005**, *24*, 2411. (i) Wang, H. M. J.; Vasam, C. S.; Tsai, T. Y. R.; Chen, S.-H.; Chang, A. H. H.; Lin, I. J. B. *Organometallics* **2005**, *24*, 486.

(4) Wang, H. M. J.; Lin, I. J. B. *Organometallics* **1998**, *17*, 972.

(5) (a) Guerret, O.; Solé, S.; Gornitzka, H.; Teichert, M.; Trinquier, G.; Bertrand, G. *J. Am. Chem. Soc.* **1997**, *119*, 6668. (b) Guerret, O.; Solé, S.; Gornitzka, H.; Trinquier, G.; Bertrand, G. *J. Organomet. Chem.* **2000**, *600*, 112.

(6) (a) Tulloch, A. A. D.; Danopoulos, A. A.; Winston, S.; Kleinhenz, S.; Eastham, G. *J. Chem. Soc., Dalton Trans.* **2000**, 4499. (b) van Veldhuizen, J. J.; Garber, S. B.; Kingsbury, S. J. S.; Hoveyda, A. H. *J. Am. Chem. Soc.* **2002**, *124*, 4954.

10.1021/om700898d CCC: $37.00 © 2007 American Chemical Society
Publication on Web 11/01/2007

Scheme 1

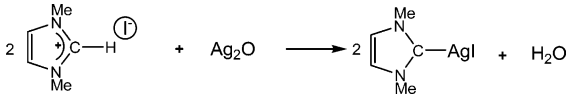

Several reasons justify the choice of the Ag_2O technique. For instance, the metalation reactions with silver oxide can be carried out in air and proceed at room temperature unless bulky imidazolium salts are employed.[6a] Moreover, no additional base is required, and the deprotonation usually takes place at the C2−H bond of the imidazolium salt. Reaction times using Ag_2CO_3 were sometimes found to be longer than when using Ag_2O.[6a] With respect to solvent, a wide variety have been used with Ag_2O employed as base: CH_2Cl_2, 1,2-dichloroethane, DMSO, MeOH, acetonitrile, and even H_2O. The fact that the silver *N*-heterocyclic carbenes can be made in water suggests that the deprotonation and subsequent metalation may be a concerted process.[2b,7] Other studies suggest that the steric bulk around the imidazolium cations affects the ability of the silver oxide to effectively deprotonate.[6a] However, although suggestions and proposals have been made regarding the possible reaction pathways, no high level computations have been performed yet to determine the mechanism of silver carbene formation.

The nature of the silver−NHC bond has been theoretically analyzed in recent publications.[8] Here, we present the results of a theoretical investigation into the mechanism of the formation of Ag(I)−NHC. The main goal of this mechanistic study is providing a rationale for the demonstrated efficiency of the silver oxide route in the synthesis of Ag−NHCs. The participation of one or two imidazolium cations along the reaction pathway will also be analyzed. A general reaction system is investigated that incorporates the *N*,*N*-dimethyl imidazolium cation and iodide as the counterion, the most popular of silver bases (Ag_2O), along with dichloromethane solvent (DCM). DFT calculations are employed to probe the mechanism, including the solvent effects of DCM using the Polarized Continuum Model (PCM).[9] The reaction studied is shown in Scheme 1.

Computational Details

Optimizations, Energies, and Solution-Phase Calculations. Density Functional Theory (DFT) calculations were performed with the Gaussian 03 software package[10] using the B3LYP functional.[11] Effective core potentials (ECPs) were used to represent the innermost electrons of silver atoms as well as the electron core of iodine atoms.[12] The basis sets for Ag and I atoms were therefore those associated with a pseudopotential[12] with a standard double-ζ LANL2DZ contraction,[10] supplemented in the case of iodine with a set of d-polarization functions.[13] The carbon, oxygen, and nitrogen atoms were described with the polarized 6-31G(d) basis set.[13] For the reactive ring hydrogen (H to be deprotonated), the 6-31G(p,d) basis set was employed.[13] The rest of the hydrogen atoms were described with a 6-31G basis set.[14]

The structures of the reactants, intermediates, transition states, and products were fully optimized in the gas phase without any symmetry restriction. Frequency calculations were performed on all optimized structures to characterize the stationary points as minima or transition states, as well as for the calculation of gas-phase Gibbs energies (G) at 298.15 K. For all of the optimized structures, the Gibbs energies of solvation were then computed in dichloromethane ($\epsilon = 8.93$) at the gas-phase optimized geometries by means of single-point calculations using the continuum PCM model.[9] Standard PCM options[10] were employed except that for the hydrogen being deprotonated, its own sphere in defining the solvent cavity had to be explicitly defined. In this way, ΔE_{DCM} (energies in dichloromethane), resulting from adding the contribution of the Gibbs energy of solvation to the gas-phase internal energies, and ΔG_{DCM} (Gibbs energies in dichloromethane), resulting from adding the contribution of the Gibbs energy of solvation coming by the continuum model to the Gibbs energies in the gas phase, were obtained.

pK_a Calculations. The deprotonation of the first azolium by Ag_2O was found to be a barrierless process in our DFT computations, while we found a barrier for the deprotonation of the second azolium by AgOH (vide infra). pK_a calculations were performed to compare the basicities of Ag_2O, AgOH, and the deprotonated imidazole carbene. A method for the accurate calculation of absolute and relative pK_a's for a series of carbenes (including the imidazole carbene studied here) in DMSO has recently been reported.[15] The absolute pK_a's of 1,3-dimethyl-imidazolium, $[Ag_2OH]^+$ and $[AgOH_2]^+$ in DMSO ($\epsilon = 46.7$) (eq 1), were calculated using an approach adopted from this work. For comparative purposes, the pK_a of $[AgOHAc]^+$ was also determined with the same computational scheme.

$$[A-H]^+_{DMSO} \rightarrow A_{DMSO} + H^+_{DMSO} \quad (A = NHC, Ag_2O, AgOH, AgOAc) \quad (1)$$

This approach requires both accurate gas-phase and solution Gibbs energies. Critical to accurate pK_a determination is the level of theory employed. For the imidazole carbene calculations, therefore, the successful methodology of Yates et al.[15] was applied. The geometries were first optimized using B3LYP and the CBSB7 basis set.[16] High level gas-phase Gibbs energies $G^0(NHC_{gas})$ and $G^0(NHC-H^+_{gas})$ were then calculated using CBS-QB3 model chemistry.[16] For the solution-phase calculations of $\Delta G^0_{DMSO}(NHC)$ and $\Delta G^0_{DMSO}(NHC-H^+)$, the polarized continuum model CPCM was used.[17] The optimum geometries from the gas-phase B3LYP/CBSB7 computations were taken and optimized at CPCM/HF/6-31+G(d) level, with standard Gibbs energy of solvation values

(7) (a) Garrison, J. C.; Simons, R. S.; Tessier, C. A.; Youngs, W. J. *J. Organomet. Chem.* **2003**, *673*, 1. (b) Kascatan-Nebioglu, A.; Panzner, M. J.; Garrison, J. C.; Tessier, C. A.; Youngs, W. J. *Organometallics* **2004**, *23*, 1928. (c) Quezada, C. A.; Garrison, J. C.; Panzner, M. J.; Tessier, C. A.; Youngs, W. J. *Organometallics* **2004**, *23*, 4846.

(8) (a) Hu, X.; Castro-Rodríguez, I.; Olsen, K.; Meyer, K. *Organometallics* **2004**, *23*, 755. (b) Nemcsok, D.; Wichmann, K.; Frenking, G. *Organometallics* **2004**, *23*, 3640. (c) Samantaray, M. K.; Roy, D.; Patra, A.; Stephen, R.; Saikh, M.; Sunoj, R. B.; Ghosh, P. *J. Organomet. Chem.* **2006**, *691*, 3797. (d) Jacobsen, H.; Correa, A.; Costabile, C.; Cavallo, L. *J. Organomet. Chem.* **2006**, *691*, 4350. (e) Díez-González, S.; Nolan, S. P. *Coord. Chem. Rev.* **2007**, *251*, 874.

(9) (a) Tomasi, J.; Persico, M. *Chem. Rev.* **1994**, *94*, 2027. (b) Amovilli, C.; Barone, V.; Cammi, R.; Cancès, E.; Cossi, M.; Menucci, B.; Pomelli, C. S.; Tomasi, J. *Adv. Quantum Chem.* **1998**, *32*, 227.

(10) Frisch, M. J.; et al. *Gaussian 03*, revision C.02; Gaussian, Inc.: Pittsburgh, PA, 2004.

(11) (a) Lee, C.; Yang, W.; Parr, R. G. *Phys. Rev. B* **1988**, *37*, 785. (b) Becke, A. D. *J. Chem. Phys.* **1993**, *98*, 5648. (c) Stephens, P. J.; Devlin, F. J.; Chabalowski, C. F.; Frisch, M. J. *J. Phys. Chem.* **1994**, *98*, 11623.

(12) (a) Wadt, W. R.; Hay, P. J. *J. Chem. Phys.* **1985**, *82*, 284. (b) Hay, P. J.; Wadt, W. R. *J. Chem. Phys.* **1985**, *82*, 299.

(13) Höllwarth, A.; Bohme, M.; Dapprich, S.; Ehlers, A.; Gobbi, A.; Jonas, V.; Kohler, K.; Stegmann, R.; Veldkamp, A.; Frenking, G. *Chem. Phys. Lett.* **1993**, *208*, 237.

(14) (a) Hehre, W.; Ditchfield, R.; Pople, J. A. *J. Chem. Phys.* **1972**, *56*, 2257. (b) Hariharan, P.; Pople, J. A. *Theor. Chim. Acta* **1973**, *28*, 213. (c) Francl, M. M.; Pietro, W. J.; Hehre, W. J.; Binkley, J. S.; Gordon, M. S.; Defrees, D. J.; Pople, J. A. *J. Chem. Phys.* **1982**, *77*, 3654.

(15) Magill, A. M.; Cavell, K. J.; Yates, B. F. *J. Am. Chem. Soc.* **2004**, *126*, 8717.

(16) Montgomery, J. A., Jr.; Frisch, M. J.; Ochterski, J. W.; Petersson, G. A. *J. Chem. Phys.* **1999**, *110*, 2822.

(17) Barone, V.; Cossi, M. *J. Phys. Chem. A* **1998**, *102*, 1995.

ΔG^0_{DMSO} then obtained by single point calculations at the CPCM/MP2/6-311+G(d,p) level. In these solvation calculations and those for Ag_2O and AgOH (vide infra), the variables TSNUM and TSARE were set at 240 and 0.3, respectively. TSNUM represents the number of tesserae on each sphere and TSARE the area of each tesserae (in Å^2). For $G^0(H^+_{gas})$, a value of -4.39 kcal mol^{-1} was taken from elsewhere,[18] likewise the $\Delta G^0_{DMSO}(H^+)$ value of -266.49 kcal mol^{-1}.[19] The difficulty of obtaining and lack of available data for these two thermodynamic quantities for a proton led us to perform our pK_a calculations in DMSO (where data were available) rather than in DCM.

To calculate the absolute pK_a of $[Ag_2OH]^+$ and $[AgOH_2]^+$, modifications to the approach used were implemented to include the DZVP all-electron basis for Ag.[20] $G^0(Ag_2O_{gas})$, $G^0(Ag_2OH^+_{gas})$, $G^0(AgOH_{gas})$, and $G^0(AgOH_2{}^+_{gas})$ Gibbs energies for Ag_2O, Ag_2OH^+, AgOH, and $AgOH_2{}^+$, respectively, were obtained by gas-phase optimizations performed using the coupled cluster CCSD method together with this Ag basis set and CBSB7 basis sets for O and H atoms.[16] For solution-phase (DMSO) Gibbs energies, the same procedure as outlined for the imidazole carbene was used (vide supra) except the full electron basis set for Ag was used in each case. $G^0(H^+_{gas})$ and $\Delta G^0_{DMSO}(H^+)$ values of -4.39 and -266.49 kcal mol^{-1}, respectively, were used as before.[18,19]

Results and Discussion

The Experimental Reaction. To perform a combined experimental and theoretical analysis of the mechanism leading to the formation of silver−NHC complexes, we first tried to perform an experimental study of the process, by following the reaction between Ag_2O and dimethyl-imidazolium iodide in DMSO-d_6 by ^{1}HNMR spectroscopy. The NMR spectra were recorded on a Varian Innova 300 MHz spectrometer.

A mixture of Ag_2O (10 mg, 0.043 mmol) and 1,3-dimethylimidazolium diiodide (9.6 and 19.3 mg, 0.086 and 0.043 mmol, respectively) was dissolved in 0.5 mL of DMSO-d_6 in an NMR tube. The reaction was monitorized by ^{1}H NMR spectroscopy using 2 mg of ferrocene as internal standard for integration purposes. The experiments were performed at different temperatures ranging from 27 to 70 °C and were recorded every 5 min during 12 h.

Silver oxide, as any other silver precursor that we could have used (Ag_2CO_3 and AgOAc), is very insoluble in all of the solvents used in the preparation of Ag−NHC complexes (pK_{sp} = 7.71, in H_2O), so that monitoring of the reaction and the determination of experimental kinetic data is seriously affected by the heterogeneous nature of the process. We thought that we could override this problem by considering that the dissolution rate of Ag_2O is greater than the reaction rate of the dissolved solute, so that the solute Ag_2O concentration is maintained constant by the solubility equilibrium and the first-order reaction becomes a pseudo-zero-order reaction with respect to silver oxide. With these considerations in mind, we performed a series of reactions in which silver oxide reacted with 1, 2, and 4 equiv of dimethylimidazolium iodide in DMSO-d_6 at a range of temperatures between 25 and 70 °C. For all of the experiments performed, a two-phase medium was obtained with a mixture of insoluble silver compounds present in the solution of the imidazolium salt and the silver−NHC products. The reactions were monitored by measuring the decrease in the signals due to the imidazolium salt (typically, the C2H proton, at δ 9.7), while the signal due to the Ag−NHC product (6.3 ppm) increases, in the presence of an internal reference of ferrocene. In all of the reactions, we observed that the reaction was almost complete (70−85% yield) after the addition of the two reactants to a NMR tube loaded with 0.5 mL of DMSO-d_6. The remaining unreacted imidazolium (30−15%) salt converted to the silver−NHC product in a slow pseudo-first-order process that we attributed only to diffusion problems that are more important when the concentration of the imidazolium salt is getting low.

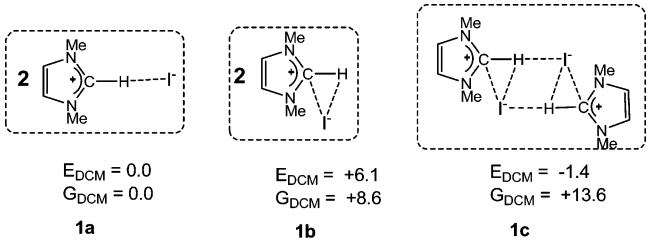

Figure 1. Optimized imidazolium−iodide ion pairs and their relative energies (E_{DCM}) and Gibbs energies (G_{DCM}) (kcal mol^{-1}) in dichloromethane.

Despite that the difficulties of getting accurate experimental kinetic data avoided the possibility of obtaining useful mechanistic information, we believe that the fact that the process is so fast implies that the formation of the products responds to an essentially barrierless pathway, probably of the type of the proton transfer between a weak acid and a base, in our case, the imidazolium salt and silver oxide. The ensuing computational study has fully confirmed this hypothesis.

Theoretical Calculations. (1) Reactants and Products. We have first analyzed the relative stabilities of the possible reactants. Several starting points have been checked in the optimization of the imidazolium−iodide ion pair, both in monomeric and in dimeric forms. Schematized in Figure 1 are the optimized monomer (**1a** and **1b**) and dimer (**1c**) forms of the reactants that were found as minima and their relative energies (E_{DCM}) and Gibbs energies (G_{DCM}) in DCM. Key geometric parameters for the optimized geometries are shown in Figure 2. With respect to energies, the associated dimer **1c** is the most favorable form for the reactants stabilized by the electrostatic interaction shown, but only 1.4 kcal mol^{-1} more stable than monomer **1a**. Considering just monomers **1a** and **1b**, **1a** is 6.1 kcal mol^{-1} more stable than **1b**. The association of the two imidazolium−iodide ion pairs is strongly disfavored by entropy, and the preference of **1c** over **1a** is reversed when G_{DCM} values are compared.

The structural characterization of silver *N*-heterocyclic carbenes has led to very different architectures depending on the synthetic conditions employed, the N-substituents, the mono- or multi-azolium nature of the salts used to react with Ag, and the coordinating or noncoordinating properties of the accompanying anions.[2,21] According to the literature, mono-azolium halides can produce Ag(I)−NHCs of various ionic or neutral structures (Figure 3). The stoichiometric reaction of short chain azolium halides in CH_2Cl_2 produces either neutral [R_2-NHC]−AgX with silver linearly bound to both a carbene and an anion (**2a**), dimers with two [R_2NHC]−Ag units connected by two bridging halides (**2d**), or ion pairs with [(R_2NHC)$_2$−

(18) Liptak, M. D.; Gross, K. C.; Seybold, P. G.; Feldgus, S.; Shields, G. C. *J. Am. Chem. Soc.* **2002**, *124*, 6421.
(19) Marcus, Y. *Pure Appl. Chem.* **1983**, *55*, 977.
(20) (a) Godbout, N.; Salahub, D. R.; Andzelm, J.; Wimmer, E. *Can. J. Chem.* **1992**, *70*, 560. (b) EMSL Basis Set Exchange, A Community Database for Computational Sciences http://gnode2.pnl.gov/bse/portal.: Schuchardt, K. L.; Didier, B. T.; Elsethagen, T.; Sun, L.; Gurumoorthi, V.; Chase, J.; Li, J.; Windus, T. L. *J. Chem. Inf. Model.* **2007**, *47*, 1045.
(21) (a) de Frémont, P.; Scott, N. M.; Stevens, E. D.; Rammnial, T.; Lightbody, O. C.; Macdonald, C. L. B.; Clyburne, J. A. C.; Abernethy, C. D.; Nolan, S. P. *Organometallics* **2006**, *24*, 6301. (b) Chiu, P. L.; Chen, C. Y.; Lee, C.-C.; Hsieh, M.-H.; Chuang, C.-H.; Lee, H. M. *Inorg. Chem.* **2006**, *45*, 2520.

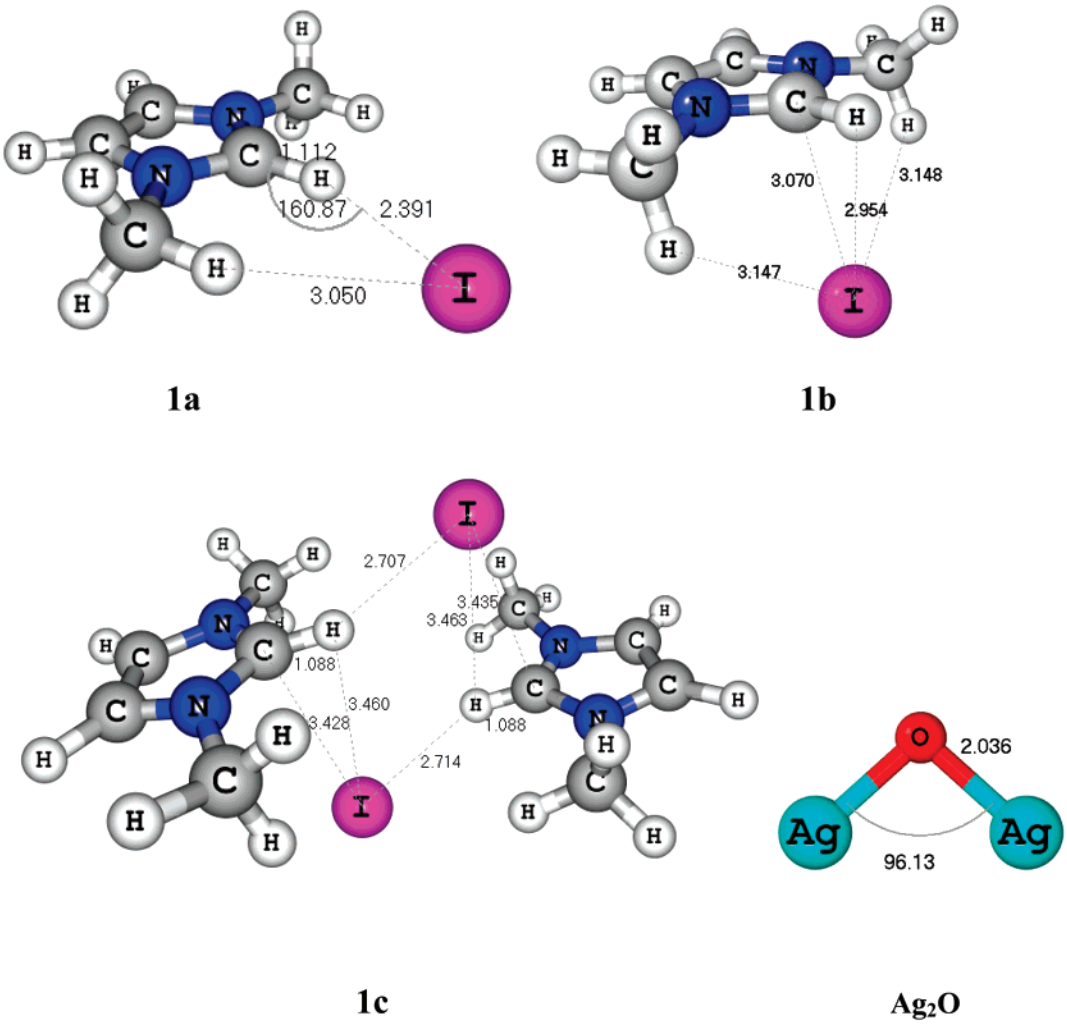

Figure 2. Key geometric parameters for reactants **1a**−**1c** and Ag_2O.

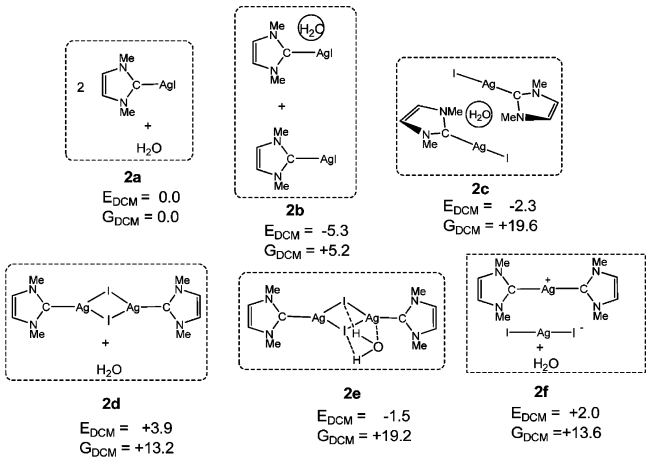

Figure 3. Possible products and their relative energies (E_{DCM}) and Gibbs energies (G_{DCM}) (kcal mol^{-1}) in dichloromethane.

Ag]$^+$ cations balanced with halogeno anions of type $[AgX_2]^-$ (**2f**).[2] Nolan et al. have recently reported the synthesis of a series of mono-carbene silver halides $[R_2NHC]$−AgCl (**2a**) and have demonstrated the influence of halide ions and the solvent on the structural formulas of Ag(I)−NHCs.[21a] Similar results have been communicated by Lee et al.[21b] Configuration **2d** has been previously reported for NHC carbene complexes of Ag with bridging halides involving a planar Ag_2−$halide_2$ cluster.[6a,22] A "butterfly" configuration for Ag_2I_2 has also been observed.[23] The conformation adopted by the $\{Ag_2X_2\}$ rings can be greatly affected by the N substituents with bulky steric substituents giving rise to a more distorted geometry.[6a,22] Ion-pair complexes (**2f**) have been obtained in the reaction of *N*,*N*′-dimethylimidazolium iodide with Ag_2O in DCM.[24] Fluxional behavior between $[R_2NHC]$−AgX and $[(R_2NHC)_2$−$Ag]^+[AgX_2]^-$ species was observed in solution for most of the complexes.[2a]

We have calculated the relative energies of species **2a**, **2d**, and **2f** in DCM solution. As a water molecule is formed in the proton by a silver substitution process, we have also considered the possibility of this water molecule interacting with the silver−NHC product (structures **2b**, **2c**, and **2e**). Shown in Figure 3 are the monomer and dimer forms of the products, and their relative energies. Key geometric parameters for the optimized geometries **2a**−**2f** are shown in Figure 4. The relative energies in DCM of **2a**, **2d**, and **2f** are of the same range, accounting for the experimental characterization of the three types of silver−NHCs depending on the experimental conditions. The dimeric structures are entropically disfavored, although the computed entropic contributions could be overestimated because they refer to gas phase and thus neglect solvation and desol-

(22) Bonnet, L. G.; Douthwaite, R. E.; Hodgson, R.; Houghton, J.; Kariuki, B. M.; Simonovic, S. *Dalton Trans.* **2004**, 3528.
(23) Pytkowicz, J.; Roland, S.; Mangeney, P. *J. Organomet. Chem.* **2001**, *631*, 157.
(24) Chen, W.; Liu, F. *J. Organomet. Chem.* **2003**, *673*, 5.

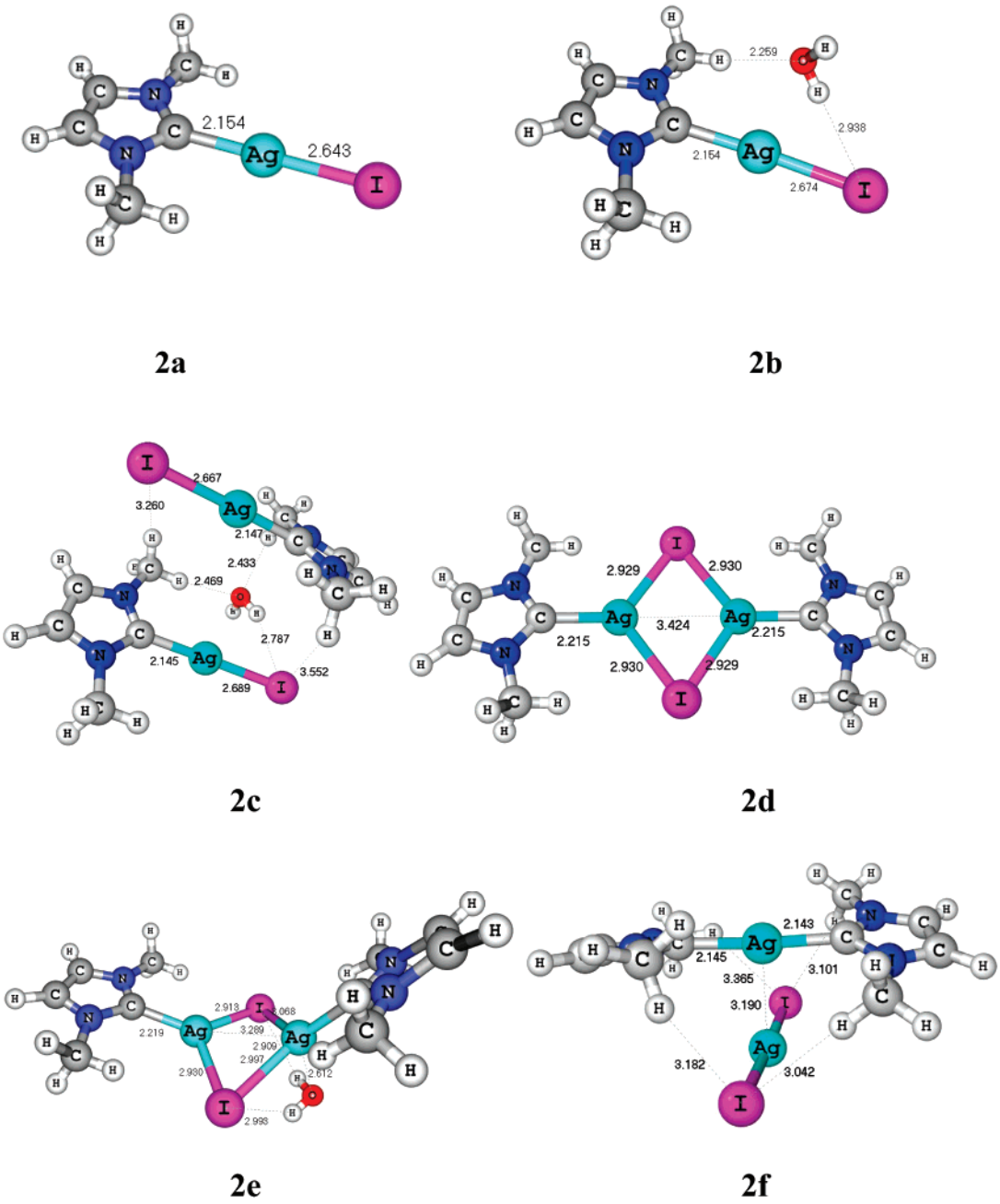

Figure 4. Key geometric parameters for possible products **2a**−**2f**.

vation effects in solution,[25] as we discuss later on. Structures incorporating a hydrogen-bonded water molecule are also disfavored in Gibbs energy terms. In **2f** there is a strong Ag−Ag interaction,[26] and the $[AgI_2]^-$ anion is oriented perpendicular to the C−Ag−C axis to maximize the interactions between the iodide atoms and the hydrogen atoms from the methyl groups. Our calculations for **2e** also show that the effect of a coordinating H_2O has a large effect on the planarity of the Ag_2I_2 cluster of **2c** and the resulting conformation adopted, in agreement with the experimentally detected structural flexibility of the Ag_2X_2 rings.[6a,22,23] Overall calculations disclose a Gibbs energy preference for the neutral monomeric form **2a** in dichloromethane solution.

(25) Recent discussions on the difficulties to calculate Gibbs energies in solution can be found in: (a) Braga, A. A. C.; Ujaque, G.; Maseras, F. *Organometallics* **2006**, *25*, 3647. (b) Tuttle, T.; Wang, D.; Thiel, W.; Köhler, J.; Hofmann, M.; Weis, J. *Organometallics* **2006**, *25*, 4504.

(26) Pyykkö, P. *Chem. Rev.* **1997**, *97*, 597.

(2) Reaction Mechanism. The reaction studied implies the deprotonation and metalation of two imidazolium cations (Scheme 1). Thus, two deprotonation and two metalation processes are required, although deprotonation and metalation could be concerted, reducing the number of steps. Several pathways have been explored for the formation of the two silver−NHC cations. In the first one, referred to as the sequential monomer pathway, only one imidazolium salt is participating in the reaction. We then checked the participation of the second imidazolium salt in the formation of the first silver−NHC (sequential dimer pathway). Both mechanisms involve the sequential formation of two silver carbenes. Another alternative also considered consists of the formation of two free NHCs, followed by metalation of these two carbenes to afford the Ag−NHC products. Finally, the direct oxidative addition of the imidazolium salt to Ag_2O was also checked as a possible alternative pathway to the silver−carbene complex.

Scheme 2. Sequential Monomer Pathway for Formation of the Two Silver Carbene Products

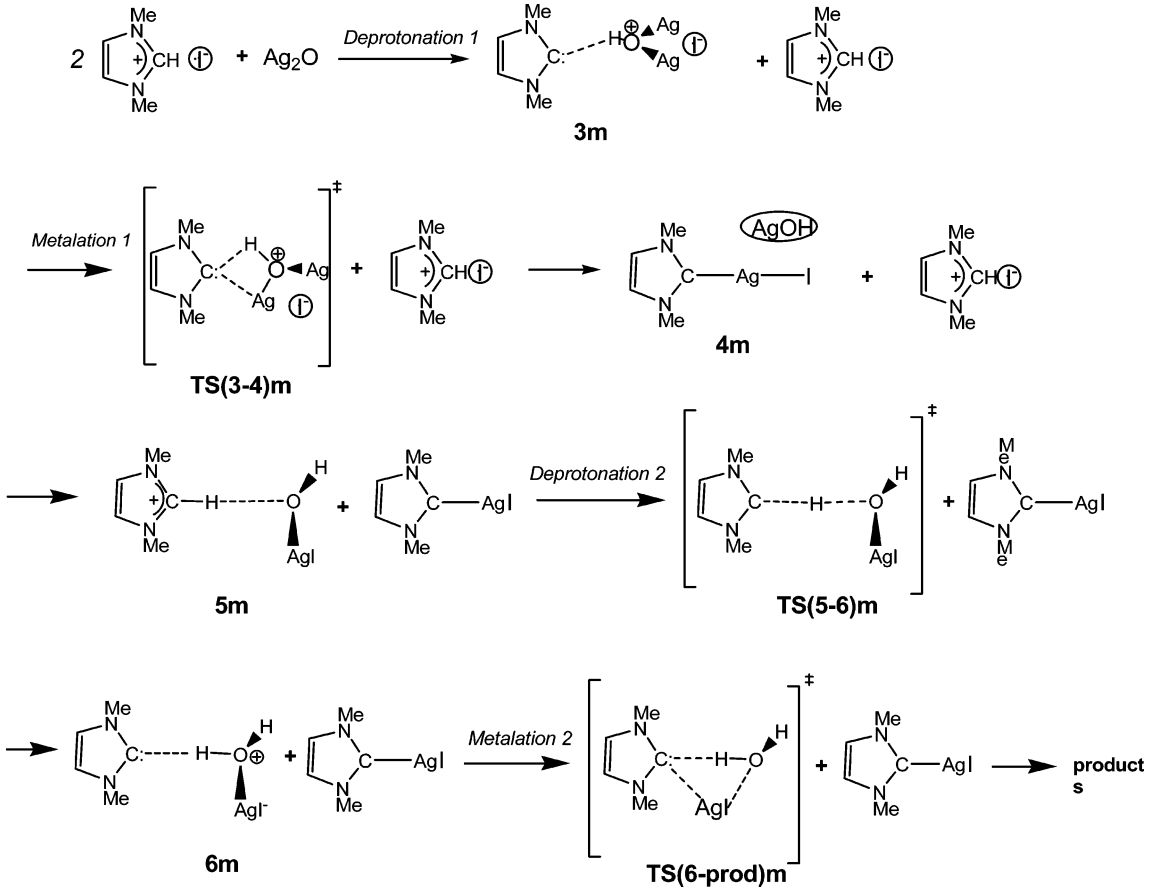

Sequential Monomer Pathway. In the sequential monomer pathway displayed in Scheme 2, we consider the mechanism to be described simply as deprotonation 1 − metalation 1 − deprotonation 2 − metalation 2, with each step occurring in that sequence. In all of the steps, only the imidazolium salt directly implied in the deprotonation/metalation processes is considered. The second imidazolium is deprotonated by AgOH. Intermediates and transition states found along the monomer pathway are labeled **m**. Note that in the following discussion from this point onward, energies referred to are Gibbs energies in solution (DCM) unless otherwise indicated.

The key geometric parameters for intermediates and transition states along this pathway and the corresponding Gibbs energy profile are displayed in Figures 5 and 6, respectively. In calculating the energetics, the lowest energy configuration for reactants (**1a**) is taken. Regarding products, **2b** is initially formed, although it then can evolve with separation of the silver−NHC molecule and water (**2a**). The reaction initiates with the barrierless abstraction of the imidazolium acidic proton (deprotonation 1) by the strong Ag_2O base, which is strongly exergonic by over 28 kcal mol^{-1}, yielding the hydrogen-bonded species **3m**. A free *N*-heterocylic carbene is easily formed in this first step. The relative acid−base strength of the imidazolium/silver oxide couple is the first driving force for the silver−NHC formation. Although in coordinating solvents Ag_2O could coordinate with solvent molecules, decreasing its basicity, the deprotonation reaction is so favored that no substantial changes in this step can be expected. Indeed, the synthesis of silver NHCs with Ag_2O has been achieved in a wide variety of solvents, some of them of coordinating nature. The barrierless nature of this first step led us to compute and compare the pK_a's of the two bases, imidazole carbene and Ag_2O (vide infra). In intermediate **3m**, the Ag−O bond aligned with the Ag−I bond is lengthened (2.17 vs 2.09 Å of the other Ag−O bond, see Figure 5), facilitating its breakage and the subsequent Ag−C bond formation (metalation 1). The Ag−Ag distance (3.01 Å) agrees with the presence of a silver(I)−silver(I) interaction in this structure.[26] The I^- counterion can also position itself so as to bridge the two silver atoms, **3′m** (Figure 5), although this form is 5.6 kcal mol^{-1} less stable than **3m** in DCM. The bridging iodide leads to longer and similar Ag−O bond lengths (2.21−2.25 Å), whereas a strong Ag−Ag interaction (2.88 Å) takes place in **3′m**.

The second step, silver transfer to the free NHC, is also a very favorable process. Formation of the silver−carbon bond (metalation 1) can occur through **TS(3−4)m** with a barrier of just 4.0 kcal mol^{-1}. Starting from **3′m** the reaction occurs through **TS(3′−4)m** with a barrier of 2.9 kcal mol^{-1}. Metalation takes place with simultaneous Ag−O bond breaking and C−Ag bond making and rupture of the $C_{carbene}\cdots HO$ hydrogen bond. The metalation step is also very exergonic (15.7 kcal mol^{-1}). The strong stabilization of the carbene by formation of the C−Ag bond constitutes a second driving force for the overall reaction.

The first two steps have led to the formation of one silver−NHC and AgOH, which will be the basis in the deprotonation of the second imidazolium. Contrary to what happens with Ag_2O, interaction of AgOH with the imidazolium salt does not produce the barrierless abstraction of the imidazolium acidic proton, but the formation of intermediate **5m** in which the proton has not been transferred yet to oxygen. This behavior is related to the weaker basic strength of AgOH and will be analyzed with pK_a calculations (vide infra). From **5m** deprotonation 2 takes place, affording intermediate **6m** after crossing the

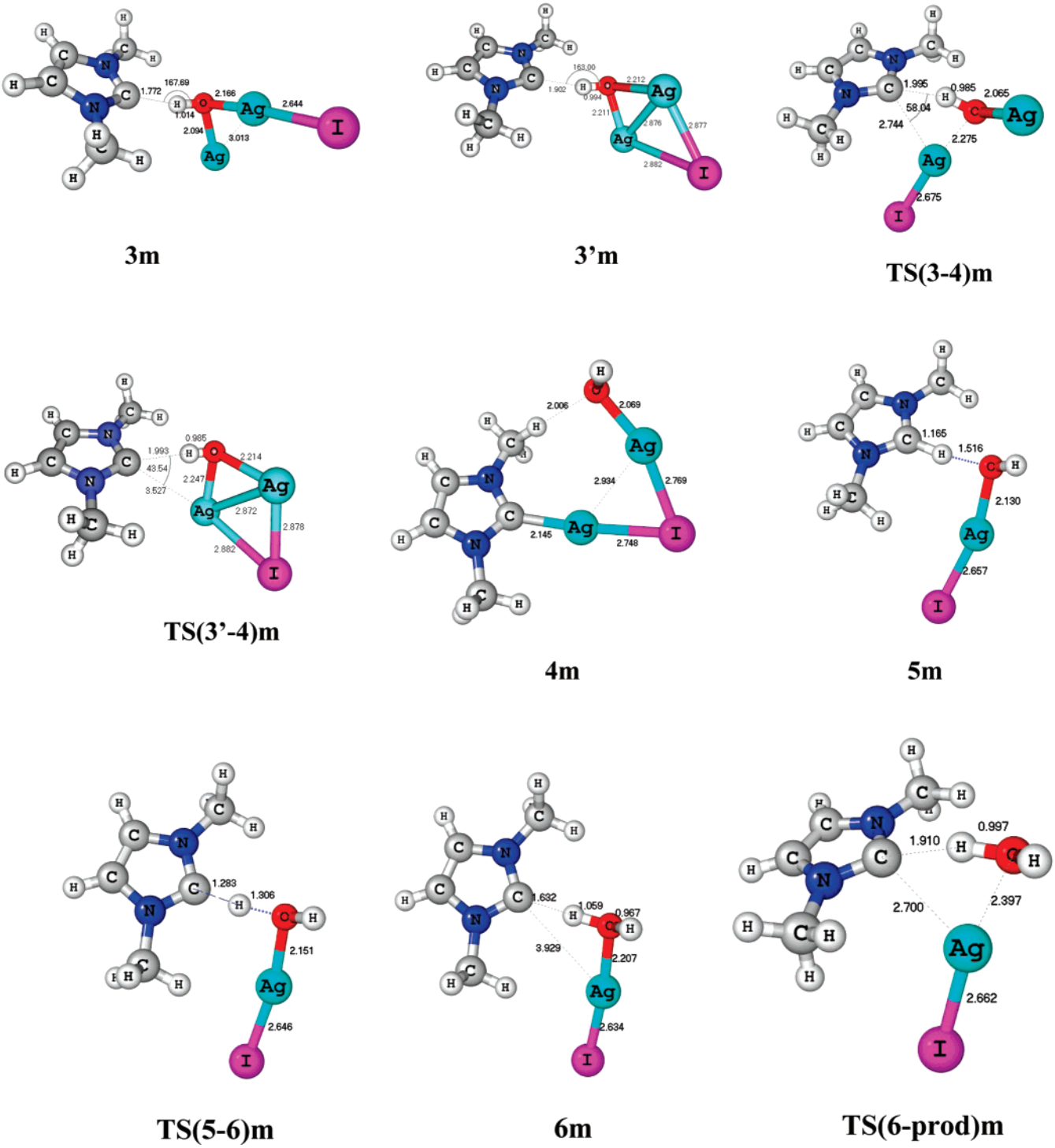

Figure 5. Structures of intermediates and transition states and key geometric parameters for the sequential monomer pathway as displayed in Scheme 2.

transition state **TS(5−6)m**. This reaction is not predicted to be exergonic in contrast to the strong exergonic first deprotonation. Indeed, the product **6m** is in fact predicted to be 1.6 kcal mol^{-1} higher in energy than the entry **TS(5−6)m**. However, such meaningless results are not unusual for single point free energy PCM calculations at gas-phase optimum geometries when differences in energies are small. The subsequent second metalation (metalation 2) then occurs with a slightly higher energy barrier (5.3 kcal mol^{-1}) than the first (4 kcal mol^{-1}), forming the second silver carbene product with the elimination of H_2O. Correspondingly, the metalation 2 reaction is less exergonic (∼10 kcal mol^{-1}) than metalation 1 (∼15 kcal mol^{-1}), although the formation of the second C−Ag bond is also a driving force for the reaction to be completed.

Metalation 2 leads to product **2b**. The thermodynamic driving force for the reaction is apparent from Figure 6. Product **2b** is found 67.8 kcal mol^{-1} below the reactants (two imidazolium salts **1a** and Ag_2O) in the Gibbs energy profile. Moreover, this product is formed through a sequence of very low barrier steps.

Sequential Dimer Pathway. We have also checked out the participation of the second imidazolium salt in the formation of the first silver−NHC. We have called this route sequential dimer pathway. To discuss the potential assistance of a second imidazolium salt in the first metalation, we consider the same

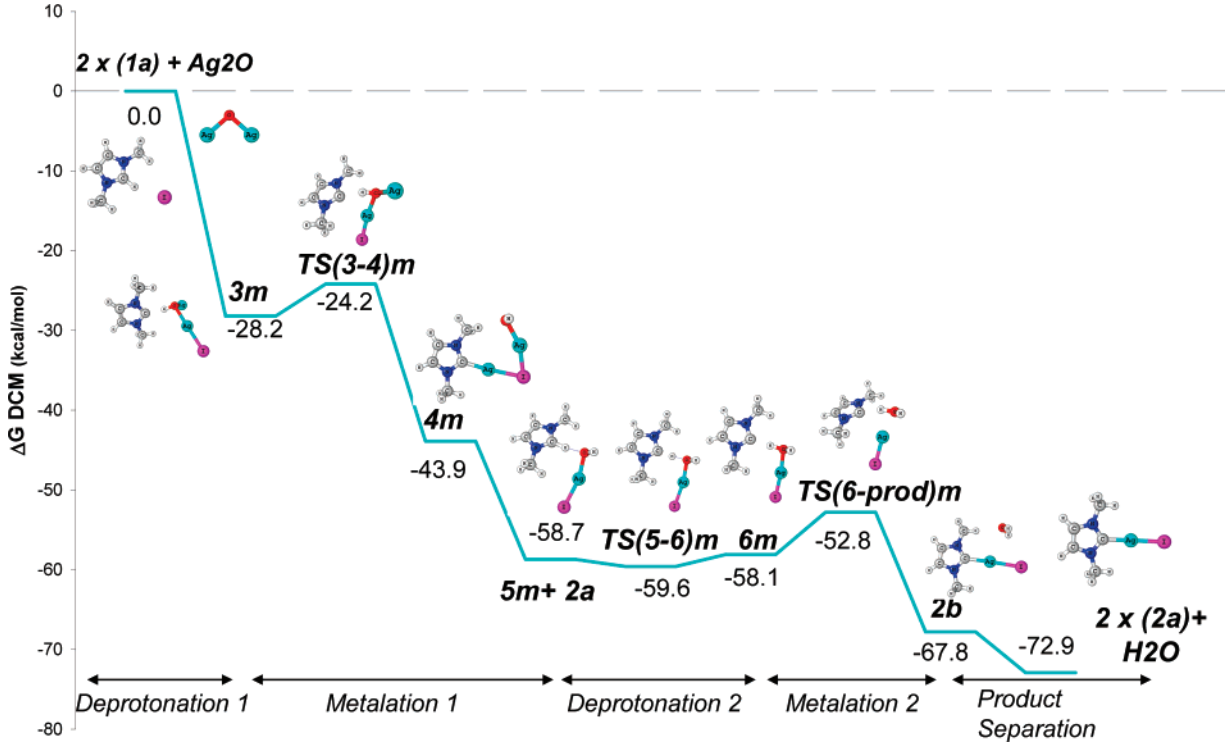

Figure 6. Gibbs energy profile (kcal mol^{-1}) in DCM for the sequential monomer pathway displayed in Scheme 2.

Scheme 3. Sequential Dimer Pathway for Formation of the Two Silver Carbene Products

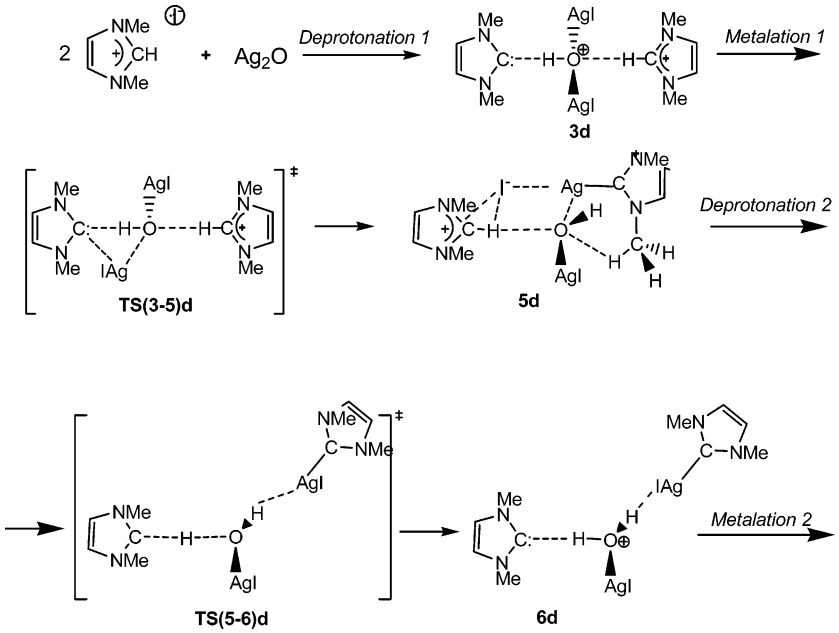

mechanism as in the sequential monomer pathway (Scheme 2), but in this case deprotonation 1 and metalation 1 are assisted by the second imidazolium (Scheme 3). Analogously, the silver−Ag first formed is present along deprotonation 2 and metalation 2 steps. Intermediates and transition states along this course are labeled **d**. Therefore, **3d** and **TS(3−4)d** are analogous to **3m** and **TS(3−4)m**, respectively, but interacting with the second imidazolium−iodide ion pair. Structures and main geometric parameters for intermediates and transition states along this pathway are shown in Figure 7 with their relative Gibbs energies displayed in Figure 8.

We see that the effect of the second imidazolium is significant. Deprotonation 1 yielding **3d** is as expected barrierless although even more exergonic (−38.9 kcal mol^{-1}) than in **3m** (−28.2 kcal mol^{-1}). Despite the unfavorable entropic contribution, the Gibbs energy of the associated species **3d** is 10.7 kcal mol^{-1} lower than that of the unassociated **3m**+**1a**, pointing out that aggregates like **3d** should be present in DCM solution. Interaction of the second imidazole/iodide ion pair also leads to similar lengthening of one of the Ag−O bond lengths in **3d** (2.15 Å) as compared to **3m** (2.17 Å). The subsequent metalation 1 through **TS(3−5)d** and a barrier of just 3.9 kcal mol^{-1} provides a low-energy route to **5d**.

As found for intermediate **3d**, the transition state for the first metalation **TS(3−5)d** is about 10 kcal mol^{-1} lower in the dimer pathway than in the monomer one. The reason of this enhanced stability is the presence in **3d** and **TS(3−5)d** of a strong hydrogen bond between the oxygen and the acidic proton of

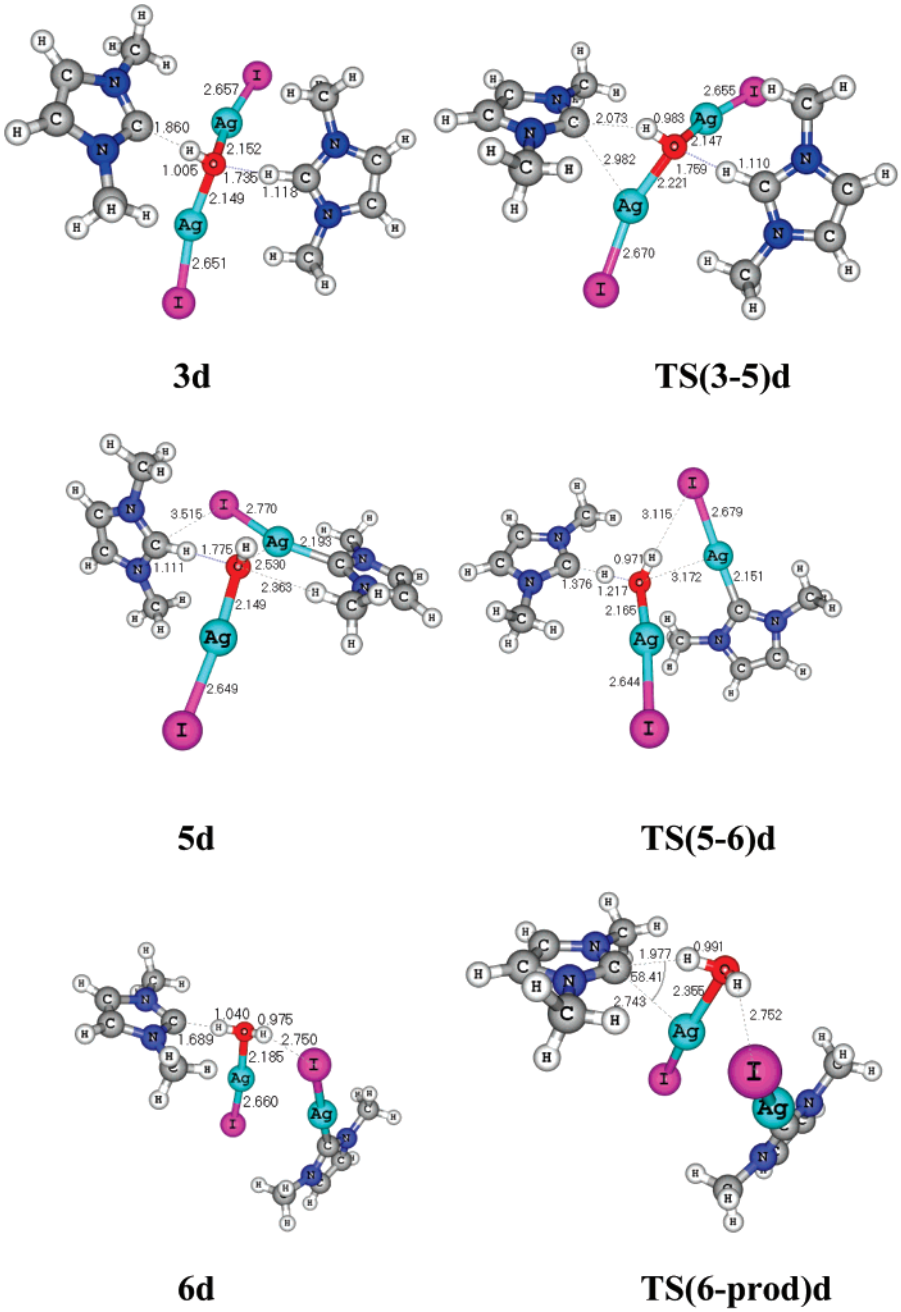

Figure 7. Structures of intermediates and transition states and key geometric parameters for the sequential dimer pathway as displayed in Scheme 3.

the second imidazolium cation. The $C_{imidazolium}$−H···OAg distance in both structures (about 1.75 Å) agrees with the presence of this interaction, which accounts for the effect of the second imidazolium in the formation of the first silver−NHC. In intermediate **5d**, we find the first silver *N*-heterocyclic carbene already formed, the silver hydroxide and the second imidazolium to be deprotonated. At this point, if we consider that the silver−NHC diffuses in the solution, this pathway connects with intermediate **5m** in the monomer pathway and deprotonation 2 and metalation 2 proceed as before (Scheme 2).

We have also contemplated in the sequential dimer pathway the possibility of assistance of the first silver−NHC in the formation of the second one. However, the presence of the first silver−NHC has very little influence in the following steps. From this point, the results in the dimer pathway are very similar to those on the monomer one. As in the monomer pathway, deprotonation 2 of the second imidazolium with the less strong silver hydroxide (AgOH) base requires 0.8 kcal mol^{-1} (**TS(5−6)d**) as compared to the barrierless deprotonation 1 using Ag_2O. Further, this reaction is not predicted to be exergonic in contrast to the strong exergonic first deprotonation. Indeed, when considering ΔG_{DCM} the product **6d** is in fact predicted to be 3.6 kcal mol^{-1} higher in energy than the entry **TS(5−6)d**. Overall, these results can be interpreted as the second deprotonation taking place with very low-energy cost in a slightly endergonic process. The subsequent second metalation (metalation 2) then occurs with a slightly higher Gibbs activation energy (5.9 kcal mol^{-1}) than the first (4.0 kcal mol^{-1}), forming the second silver carbene molecule with the concomitant elimination of H_2O. Correspondingly, the metalation 2 reaction is less strongly exothermic (∼9 kcal mol^{-1}) overall than metalation 1 (∼16 kcal mol^{-1}), although the stabilization of the system after formation of the second C−Ag bond is also a

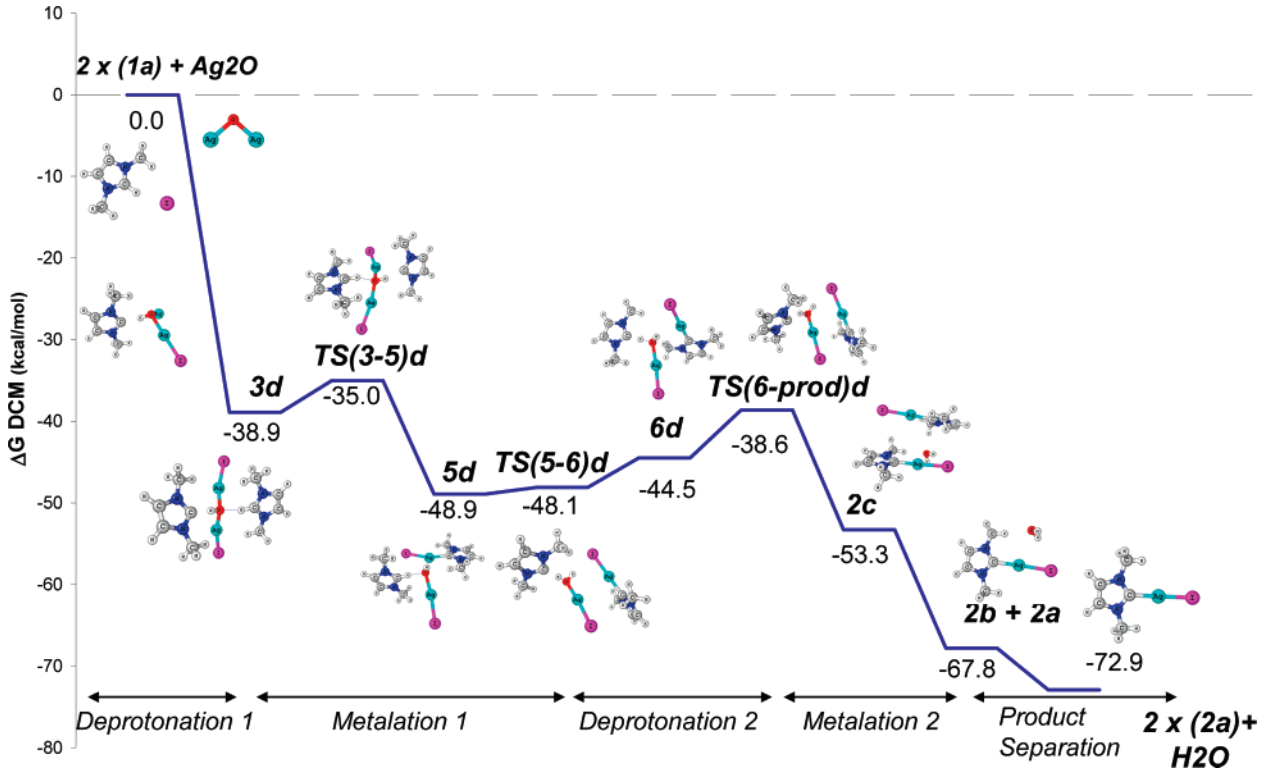

Figure 8. Gibbs energy profile (kcal mol^{-1}) in DCM for the sequential dimer pathway displayed in Scheme 3.

driving force for the reaction to be complete. In this way, product **2c** is formed through a sequence of very low barrier steps. This product is found 53.3 kcal mol^{-1} below the reactants (two imidazolium salts **1a** and Ag_2O) in the Gibbs energy profile. **2c** can evolve to the final product **2a** with separation of the two silver−NHC molecules and water.

Comparison of the Gibbs energy profiles for the sequential monomer and dimer pathways shows that the favored route for the formation of the two silver *N*-heterocyclic carbenes involves a barrierless and very exergonic deprotonation of the first imidazolium followed by a low barrier and also exergonic metalation, affording the first silver−NHC. The second imidazolium assists these two steps stabilizing intermediates and the transition state by the formation of a strong $C_{imidazolium}$−H···OAg hydrogen bond. The formed [R_2NHC]−AgI then diffuses in the solution and silver hydroxide deprotonates the second imidazolium salt in a slightly endergonic process. After metalation, the second silver−NHC is obtained. In summary, therefore, deprotonation 1 and metalation 1 follow the steps associated with the sequential dimer pathway, while the most favored steps for deprotonation 2 and metalation 2 are those associated with the sequential monomer pathway (Figure 9).

Up to this point, we have considered the Gibbs energies of reaction and activation in DCM (ΔG_{DCM}), obtained adding to the Gibbs energies in gas phase the contribution of the Gibbs energy of solvation coming by the continuum model. Thus, the computed entropic contributions refer to gas phase and neglect solvation and desolvation effects in solution. It is a subject under current discussion of how the entropic effects can be taken into account in solution calculations.[25] Entropic contributions arising from gas-phase calculations can overestimate the real solution values because in solution the entropic effects will be less pronounced due to solvation and desolvation. To assess the importance of entropic effects in the mechanism, we also report in Figure 9 a comparison between the ΔG and ΔE profiles in dichloromethane. As the origin of energies is two molecules of the imidazolium salt **1a** and Ag_2O, with the three molecules infinitely apart, the association reactions suffer from an entropic penalty, while dissociation reactions are entropically favored. The ΔE_{DCM} profile has the same general shape as the ΔG_{DCM} one. However, the species corresponding to the dimer pathway (from **3d** to **5d**) are placed about 25 kcal mol^{-1} lower than in the ΔG_{DCM} profile. This difference is reduced to about 10 kcal mol^{-1} in the steps corresponding to the monomer pathway (from **5m** to **2b**+**2a** product). Conversely, water dissociation in the product (from **2b** to **2a**) is favored in the ΔG_{DCM} profile but unfavorable in the ΔE_{DCM} one. Comparison of ΔE_{DCM} values for the monomer and dimer pathways shows that, while the relative energy of the species leading to the first silver−NHC is considerably lowered when introducing the second imidazolium, the energies of intermediates and transition states related to the formation of the second silver−NHC are very similar without or with the presence of the first silver−NHC. These results show that there is no significant stabilization in the system due to the interaction with the first silver−NHC. On the whole, the conclusions about the feasibility of the proposed pathway and the driving force for the reaction are the same in energy and Gibbs energy grounds.

Deprotonation of Both Imidazoliums. We have also analyzed a mechanism in which the two deprotonations first occur, generating two free NHCs, sequentially followed by metalations of these two carbenes. Although the overall process formally implies the same reaction steps (two deprotonations and two metalations), this pathway follows a different mechanism as compared to the one described before, in the sense that the order of the steps has been altered to: deprotonation 1 − deprotonation 2 − metalation 1 − metalation 2 (Scheme 4). This mechanism implies the simultaneous participation of both imidazolium salts and can be described as the sequential deprotonation−sequential metalation dimer pathway. Key geometric parameters of the new structures introduced by this scheme are shown in Figure 10.

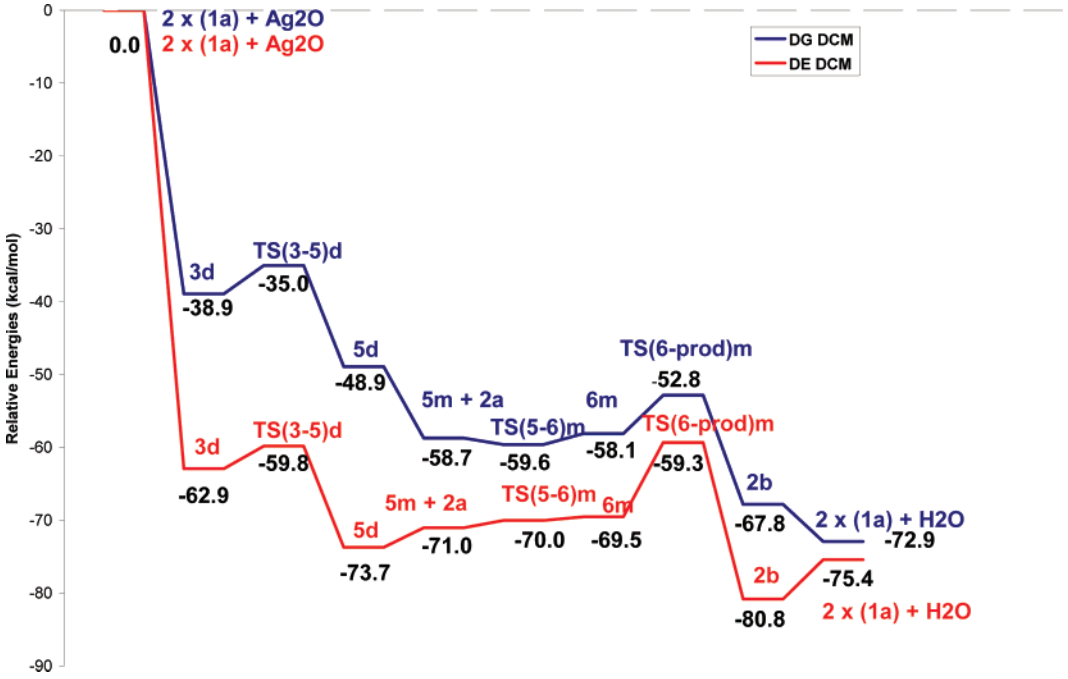

Figure 9. Comparison between ΔG_{DCM} (blue line) and ΔE_{DCM} (red line) profiles for the most favored route for the formation of the two silver *N*-heterocyclic carbenes.

Scheme 4. Sequential Deprotonation−Sequential Metalation Dimer Pathway for Formation of the Two Ag Carbene Products

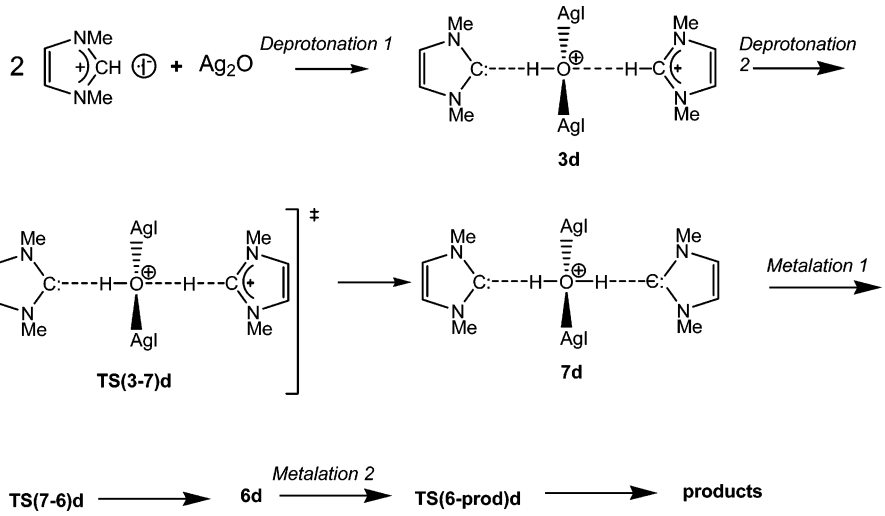

The reaction initiates with the barrierless and strongly exergonic deprotonation 1 (−38.9 kcal mol^{-1}) affording intermediate **3d**, already discussed. It is then followed by the less favorable deprotonation 2 (barrier = +4.9 kcal mol^{-1}) through **TS(3−7)d** to intermediate **7d**, which has the same Gibbs energy as **TS(3−7)d**. **3d** → **7d** is an endergonic reaction by >4 kcal mol^{-1}. Deprotonation 2 leads to a lengthening of the Ag−O bonds, from 2.15 Å in **3d** to 2.22 Å in **7d**. In intermediate **7d**, two free carbenes are linked by a water molecule that is bridging two AgI units, thus entailing a four-coordinated oxygen atom. According to this feature, **7d** is an unstable species. An alternative product (**8d**, Figure 10) for the sequential first and second deprotonations was located, but this intermediate is even higher in Gibbs energy than **7d** by 13.8 kcal mol^{-1}. **8d** presents a structure for the Ag_2I_2 unit similar to that of **3′m** with an Ag−Ag bond. **TS(3−7)d** and **7d** lie at the same Gibbs energy level, and what happens from **TS(3−7)d** to **7d** is a near free motion of a proton between the carbon and oxygen atoms. Intermediate **6d** would be the product from metalation of **7d**. It lies 10.5 kcal mol^{-1} below **7d**. In principle, it seems possible obtaining **6d** from **7d** (metalation 1). From **6d** and then through **TS(6-prod)d**, product **2c** would be formed (metalation 2) (a step already discussed). However, despite an extensive exploration of the potential energy surface, we did not locate the transition state for metalation 1 (**TS(7−6)d**), which should connect **7d** with **6d**. All of the attempts to find a transition state in this region have reverted to **(TS3−7)d**. Indeed, this is a very flat region of the potential energy surface. We have found that, starting from **7d**, in which the C−Ag distance is about 3.9 Å, the silver can approach more than 1 Å to the carbon with the energy increasing less than 2 kcal mol^{-1}. Starting then from the point at 2.8 Å in the C−Ag reaction coordinate and optimizing without constrains intermediate **5d**, containing an Ag−NHC already formed, a free carbene and the [HOAg−I]$^-$ base are attained. Metalation of one carbene can take place in **7d**, but it is accompanied by a very easy transfer of a proton back to the C atom of the other carbene. Thus, a mechanism

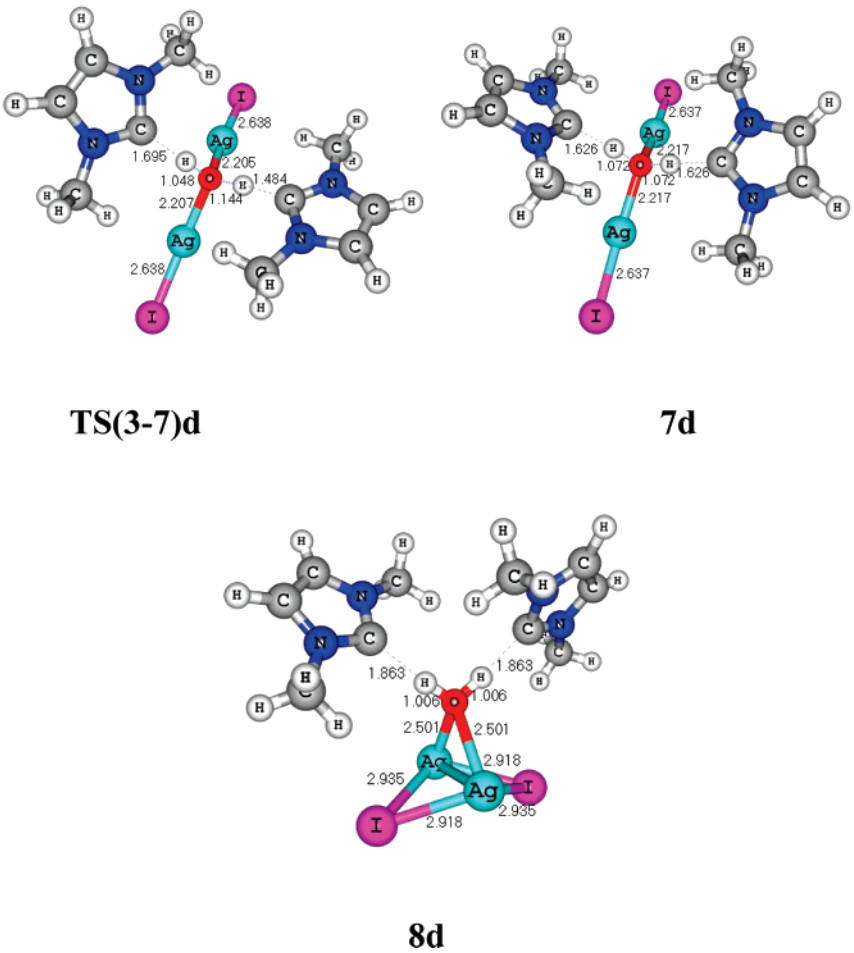

Figure 10. Key geometric parameters for **TS(3−7)d** and intermediates **7d** and **8d**.

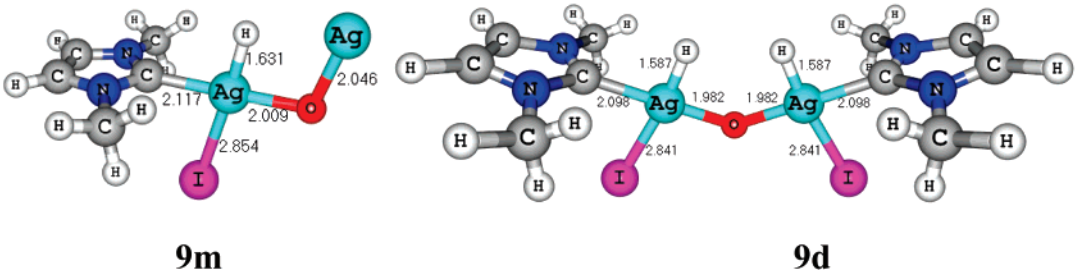

Figure 11. Intermediates formed by oxidative addition in monomer (**9m**) and dimer (**9d**) pathways.

consisting of two deprotonation steps followed by two metalation steps is not likely.

Oxidative Addition Pathway. The oxidative addition of 2-methylimidazolium salts to low valent group 10 metals has been studied from the experimental and theoretical points of view.[27] In fact, the reaction is the reverse of the ubiquitous reductive elimination reaction observed for hydrocarbonyl−Pd−NHC complexes.[28] More recently, the C2−H oxidative addition of imidazolium salts has been validated for other metals such as Rh and Ir,[29] thus widening the scope of this reaction by converting the process to a valid synthetic procedure to NHC complexes. To discard the direct oxidative addition of the imidazolium salt to Ag_2O as a possible alternative pathway to the silver−carbene complexes, this mechanism was also checked but abandoned due to the unstable nature of the potential product intermediates. Figure 11 shows the intermediates formed via monomer and dimer oxidative addition pathways, respectively. Formation of the monomer intermediate **9m** is endergonic by 43.6 kcal mol^{-1} in the DCM solution when compared to the reactants. Formation of the dimer **9d** is over twice that value (+97.0 kcal mol^{-1}).

(3) pK_a Calculations. As mentioned above, due to the barrierless nature of the deprotonations with Ag_2O base, pK_a calculations in DMSO were performed to compare the pK_a's of Ag_2O and the imidazole carbene studied in the reaction. A first

(27) (a) McGuinness, D. S.; Cavell, K. J.; Yates, B. F.; Skelton, B. W.; White, A. H. *J. Am. Chem. Soc.* **2001**, *123*, 8317. (b) McGuinness, D. S.; Cavell, K. J.; Yates, B. F. *Chem. Commun.* **2001**, 355. (c) Duin, M. A.; Clement, N. D.; Cavell, K. J.; Elsevier, C. J. *Chem. Commun.* **2003**, 400. (d) Cavell, K. J.; McGuinness, D. S. *Coord. Chem. Rev.* **2004**, *248*, 671. (e) Clement, N. D.; Cavell, K. J.; Jones, C.; Elsevier, C. J. *Angew. Chem., Int. Ed.* **2004**, *43*, 1277.

(28) (a) McGuinness, D. S.; Green, M. J.; Cavell, K. J.; Skelton, B. W.; White, A. H. *J. Organomet. Chem.* **1998**, *565*, 165. (b) McGuinness, D. S.; Cavell, K. J.; Skelton, B. W.; White, A. H. *Organometallics* **1999**, *18*, 1596.

(29) (a) Viciano, M.; Mas-Marza, E.; Poyatos, M.; Sanau, M.; Crabtree, R. H.; Peris, E. *Angew. Chem., Int. Ed.* **2005**, *44*, 444. (b) Viciano, M.; Poyatos, M.; Sanau, M.; Peris, E.; Rossin, A.; Ujaque, G.; Lledós, A. *Organometallics* **2006**, *25*, 1120.

indication of the relative basicities of carbene and silver oxide and silver can be obtained computing the gas-phase proton affinities (PA) of both molecules. The PA of 1,3-dimethylimidazol-2-ylidene has been calculated at different computational levels.[15,30] Values obtained range between 258.3 and 261.8 kcal mol^{-1}. Our value, using the CBS-QB3 level of calculation, which is expected to provide very accurate thermochemical results, is 258.9 kcal mol^{-1}, in agreement with the PA reported by Yates and col.[15] We have computed a PA of 297.4 kcal mol^{-1} for Ag_2O. These gas-phase results indicate that silver oxide presents a notably higher proton affinity than 1,3-dimethylimidazol-2-ylidene. Evaluation of the pK_a's of the conjugate acids of the carbene (the imidazolium cation) and the silver oxide (Ag_2OH^+) in DMSO has fully confirmed the gas-phase results.

A proven accurate method[15] for theoretical prediction of pK_a's for the conjugate acids of carbenes was adopted for the imidazolium cation and a modified version of this approach used for Ag_2O to accommodate an all-electron basis set for the silver atom.

The pK_a of a HA^+/A system can be theoretically determined using the following thermodynamic cycle:

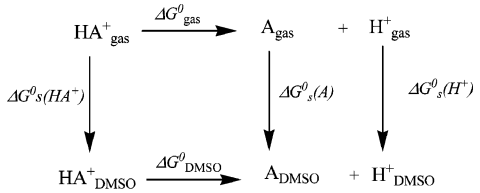

Here, ΔG^0_{gas} and ΔG^0_{DMSO} represent the Gibbs energy of deprotonation in the gas and solution phases, respectively, and $\Delta G^0_s(X)$ represents the Gibbs energy of solvation of species X.

The Gibbs reaction energy in DMSO is computed from:

$$\Delta G^0_{DMSO} = G^0(A_{DMSO}) + G^0(H^+_{DMSO}) - G^0(HA^+_{DMSO})$$
$$= G^0(A_{gas}) + \Delta G^0_{DMSO}(A) + G^0(H^+_{gas}) + \Delta G^0_{DMSO}(H^+) - G^0(HA^+_{gas}) - \Delta G^0_{DMSO}(HA^+)$$

and then:

$$pK_a = \Delta G^0_{DMSO}/2.303RT$$

Using these equations, the pK_a of $[NHC-H]^+$ (1,3-dimethylimidazolium) in DMSO was computed as 21.3. Yates et al. obtained a value of 20.9 using the same method, but also an average of 21.1 for the four different methods employed.[15] Meanwhile, we obtained a value of 24.2 for the pK_a of $[Ag_2OH]^+$. The exact accuracy of this value is unclear; however, a high level of theory (CCSD) and large all-electron basis set for Ag was employed for the calculations, giving credibility to the result obtained.

We have also calculated the Gibbs reaction energy in DMSO of the acid−base reaction:

$$[NHC-H]^+ + Ag_2O \rightarrow NHC + [Ag_2OH]^+ \qquad (2)$$

According to the large ΔpK_a between both conjugated acids, this reaction is very exergonic: $\Delta G^0_{DMSO} = -44.7$ kcal mol^{-1}. This value is not far from that calculated for the barrierless first deprotonation step in the sequential deprotonation−metalation pathway. The ΔpK_a of three units between the imidazolium cation and the conjugated acid of Ag_2O is the driving force for starting the reaction.

We have found a very different behavior for the second deprotonation, which is performed by AgOH. This process is slightly endergonic, and no stabilization of the system results from deprotonation of the second imidazolium. To address this point, we have also calculated the pK_a of silver hydroxide using the same procedure as above. The gas-phase proton affinity of AgOH (259.4 kcal mol^{-1}), considerably lower than that of Ag_2O and close to that of 1,3-dimethyl-imidazolium, gives a first clue about the behavior of silver hydroxide as a base. From the thermodynamic cycle depicted above, we have estimated a value of 21.2 for the pK_a of $[AgOH_2]^+$, three units below that of $[Ag_2OH]^+$ and very close to that of the imidazolium (21.3). In agreement with the very low pK_a difference between $[NHC-H]^+$ and $[Ag_2OH]^+$, the Gibbs reaction energy in DMSO of the acid−base reaction:

$$[NHC-H]^+ + AgOH \rightarrow NHC + [AgOH_2]^+ \qquad (3)$$

is small (−1.6 kcal mol^{-1}). Thus, the deprotonation of the second imidazolium salt, performed by AgOH, is not contributing to the stabilization of the system as the first one does.

To compare the behavior of silver oxide with other commonly used silver bases, we have also computed, following the same computational scheme, the pK_a of $[AgOHAc]^+$. The gas-phase proton affinity of AgOAc is 233.5 kcal mol^{-1}, notably lower than that of 1,3-dimethylimidazol-2-ylidene (258.9 kcal mol^{-1}). The estimated pK_a of $[AgOHAc]^+$ in DMSO is 3.3, much lower than that of imidazolium. Despite that the result obtained may seem obvious because AcOH is the conjugated acid of AgOAc, the calculation is useful because it validates the accuracy of the methodology employed in the pK_a calculations.

The Gibbs reaction energy in DMSO of the acid−base reaction:

$$[NHC-H]^+ + AgOAc \rightarrow NHC + [AgOHAc]^+ \qquad (4)$$

is +24.2 kcal mol^{-1}. Comparing this value with those obtained with Ag_2O and AgOH, a very different energy profile for the deprotonation step can be expected: a highly exergonic process turns into a substantially endergonic one. The high basicity of silver oxide appears to be mainly responsible for its efficiency in the silver *N*-heterocyclic carbene formation.

Conclusions

DFT computations have been used to investigate the mechanism of silver *N*-heterocyclic carbene formation using a silver base (Ag_2O). The reaction studied requires two deprotonations and two metalations. The exploration of several mechanistic possibilities has shown that the most favorable pathway consists of the sequence of deprotonation 1 − metalation 1 − deprotonation 2 − metalation 2 steps. The second imidazolium salt assists the formation of the first silver−NHC by formation of a strong $C_{imidazolium}$−H···OAg hydrogen bond. The overall reaction is thermodynamically driven, all of the steps taking place with very low Gibbs activation energies. Conversion of two imidazolium salts to two silver carbenes entails a system stabilization of more than 70 kcal mol^{-1}. The first driving force for the reaction is the ΔpK_a between $[NHC-H]^+$ and $[Ag_2OH]^+$ acids (more than 3 pK_a units). The high basicity of Ag_2O as compared to imidazole leads to barrierless deprotonation of

(30) (a) Graham, D. C.; Cavell, K. J.; Yates, B. F. *J. Phys. Org. Chem.* **2005**, *18*, 298. (b) Martin, D.; Illa, O.; Baceiredo, A.; Bertrand, G.; Ortuño, R. M.; Branchadell, V. *J. Org. Chem.* **2005**, *70*, 5671.

the first imidazolium, with a ΔG for this acid−base reaction of about −50 kcal mol^{-1}. Further stabilization of the system (about 10 kcal mol^{-1}) is attained by silver transfer to the free NHC formed in the deprotonation step. The strong stabilization of the carbene by formation of the C−Ag bond constitutes a second driving force for the overall reaction. The first two steps have led to the formation of one silver−NHC molecule in a highly exergonic process (ΔG about −60 kcal mol^{-1}). Formation of the second silver−NHC further stabilizes the system, although in minor extension (about 10 kcal mol^{-1}). This stabilization comes entirely from the metalation step. The pK_a of $[AgOH_2]^+$ is very close to that of the imidazolium, and deprotonation of the second $[NHC-H]^+$ by AgOH is an almost thermoneutral equilibrium that does not contribute to the system stabilization.

Silver−NHC complexes are a family of important compounds due to their recent use in the preparation of many transition metal *N*-heterocyclic carbenes. Despite that there is a large number of publications regarding the preparation and the structural diversity of such compounds,[2] and the theoretical determination of the nature of the Ag−NHC bond,[8] our work is the first theoretical study focused on determining the mechanism of their formation. Also, we have also rationalized the formation of the different types of Ag−NHC complexes based on their topology and nuclearity, and we explained the different geometric parameters according to intermetallic, solvent, and counterion interactions. Based on these studies, the monomeric compound NHC−Ag−I, **2a**, in which the two ligands adopt a linear disposition, seems to be the most favorable species in CH_2Cl_2 solution.

Our results may explain some experimental observations previously reported. For example, it is known that the kinetics of Ag−NHC formation of bis- and tris-imidazolium salts is slower than the same process using mono-imidazolium salts.[5a] Because we found the formation of the first Ag−NHC is assisted by a second imidazolium salt, topological restrictions on the bis- and trisimidazolium compounds may prevent this process from occurring and hence provide slower kinetics. Other experimental consequences may be envisaged from our studies, and, in fact, we undoubtedly believe that further study is needed to provide further insight into the factors that control the formation of these useful compounds.

Acknowledgment. We gratefully acknowledge financial support from the MEC of Spain (projects CTQ2005-05817 and CTQ2005-09000-C02-01). A.L. thanks the Generalitat de Catalunya for a Distinció per a la Promoció de la Recerca Universitària. J.M.H. acknowledges the European Commission for financial support via the TMR network grant "HYDROCHEM" (HPRN-CT-2002-00176).

Supporting Information Available: Complete ref 10. Cartesian coordinates and gas phase and DCM potential and Gibbs energies of all optimized structures, together with the all-electron basis set for Ag and thermodynamical data employed in the pK_a calculations. This material is available free of charge via the Internet at http://pubs.acs.org.

OM700898D